Breaking of Galilean Invariance in the Hydrodynamic Formulation of Ferromagnetic Thin Films

Ezio Iacocca,[1,2,*] T. J. Silva,[3] and Mark A. Hoefer[1]

[1]*Department of Applied Mathematics, University of Colorado, Boulder, Colorado 80309-0526, USA*
[2]*Department of Physics, Division for Theoretical Physics, Chalmers University of Technology, 412 96 Gothenburg, Sweden*
[3]*National Institute of Standards and Technology, Boulder, Colorado 80305-3328, USA*

Microwave magnetodynamics in ferromagnets are often studied in the small-amplitude or weakly nonlinear regime corresponding to modulations of a well-defined magnetic state. However, strongly nonlinear regimes, where the aforementioned approximations are not applicable, have become experimentally accessible. By reinterpreting the governing Landau-Lifshitz equation of motion, we derive an exact set of equations of dispersive hydrodynamic form that are amenable to analytical study even when full nonlinearity and exchange dispersion are included. The resulting equations are shown to, in general, break Galilean invariance. A magnetic Mach number is obtained as a function of static and moving reference frames. The simplest class of solutions are termed uniform hydrodynamic states (UHSs), which exhibit fluidlike behavior including laminar flow at subsonic speeds and the formation of a Mach cone and wave fronts at supersonic speeds. A regime of modulational instability is also possible, where the UHS is violently unstable. The hydrodynamic interpretation opens up novel possibilities in magnetic research.

Magnetodynamics in thin film ferromagnets has been studied for many decades. Advances in nanofabrication and the advent of spin transfer [1,2] and spin-orbit torques [3] have opened a new frontier of experimentally accessible nonlinear physics [4–8]. Large-amplitude excitations negate the use of typical linear or weakly nonlinear analyses [9–11], necessitating instead either micromagnetic simulations [12] or analytical approaches suited to strongly nonlinear dynamics. Therefore, an interpretation of the Landau-Lifshitz (LL) equation that includes full nonlinearity, yet is amenable to analytical study, would be insightful.

A hydrodynamic interpretation was proposed by Halperin and Hohenberg [13] to describe spin waves in anisotropic ferro- and antiferromagnets. Recently, theoretical studies of thin film ferromagnets with planar anisotropy have identified a relationship to superfluidlike hydrodynamic equations [14–19] supporting large-amplitude modes beyond weakly nonlinear spin wave and macrospin modes [10,11]. However, these studies are limited to the long-wavelength, low-frequency regime where linear and weakly nonlinear approaches apply. The relaxation of these approximations along with the identification of a deep connection between magnetodynamics and fluid dynamics brings new perspectives on magnetism and reveals novel physical regimes. Indeed, nonlinear, dispersive physics are required to describe superfluids and exotic structures such as solitons, quantized vortices, and dispersive shock waves (DSWs) [20–23], as exemplified by Bose-Einstein condensates (BECs) [20–22,24–34]. To obtain an analytical description of large-amplitude magnetic textures, we introduce dispersive hydrodynamic (DH) equations for a thin-film ferromagnet.

This Letter shows that the LL equation exactly maps into a DH system of equations, without long-wavelength and low-frequency restrictions. The conservative equations are analogous to the Euler equations of a compressible, isentropic fluid. The DH equations for a planar ferromagnet admit spin-current-carrying, spatially periodic magnetization textures termed "uniform hydrodynamic states" (UHSs), providing a continuous interpolation between large amplitude spin superflows [14–16] and small-amplitude spin waves. Within the DH formulation, we prove that planar ferromagnets break Galilean invariance and elucidate their reference-frame-dependent dynamics by identifying the linear dispersion relation for spin waves propagating on top of a UHS background. Such symmetry breaking at the level of linear spin waves is striking and fundamentally different from the nontrivial speed-dependent dynamics of topological textures due to their inherent nonlinearity, e.g., Walker breakdown for domain wall propagation [35] and core reversal in magnetic vortices [36]. In this Letter, we also show that static textures can break Galilean invariance for infinitesimal spin wave excitations that ride on a textured background. To emphasize this novel result, we suggest a Brillouin light scattering experimental test where broken Galilean invariance manifests itself as a spin-wave dispersion shift in the presence of a UHS.

We consider the nondimensionalized LL equation (see Supplemental Material [37])

$$\frac{\partial \mathbf{m}}{\partial t} = -\mathbf{m} \times \mathbf{h}_{\text{eff}} - \alpha \mathbf{m} \times \mathbf{m} \times \mathbf{h}_{\text{eff}}. \quad (1)$$

Damping is parametrized by the Gilbert constant α, $\mathbf{m} = \mathbf{M}/M_s = (m_x, m_y, m_z)$ is the magnetization vector

normalized to the saturation magnetization, and $\mathbf{h}_{\mathrm{eff}} = \Delta\mathbf{m} - \sigma m_z \hat{\mathbf{z}} + h_0 \hat{\mathbf{z}}$ is the normalized effective field including ferromagnetic exchange, $\Delta\mathbf{m}$; total anisotropy determined by $\sigma = \mathrm{sgn}(M_s - H_k)$, where H_k is the perpendicular magnetic anisotropy field, such that $\sigma = +1$ ($\sigma = -1$) represents a material with easy-plane (perpendicular magnetic) anisotropy; and a perpendicular applied field, $h_0 \hat{\mathbf{z}}$. This nondimensionalization of a two-dimensional (2D) thin film provides a parameter-free description of materials with planar or uniaxial anisotropy. We consider an idealized case where in-plane magnetic anisotropy is negligible; i.e., its symmetry-breaking contribution only perturbs the leading order solution, similar to domain wall Brownian motion [40].

Fluidlike variables are introduced using the canonical Hamiltonian cylindrical transformation [41]

$$n = m_z, \qquad \mathbf{u} = -\nabla\Phi = -\nabla[\arctan(m_y/m_x)], \qquad (2)$$

where Φ is the azimuthal phase angle. We identify n ($|n| \leq 1$) as the longitudinal spin density and $\mathbf{u}$ as the fluid velocity. There are two important features of Eq. (2). First, the flow is irrotational because the velocity originates from a phase gradient, i.e., only quantized circulation, such as a magnetic vortex [15], is possible. Second, Φ is undefined when $n = \pm 1$, corresponding to fluid vacuum.

Utilizing the transformation (2) and standard vector calculus identities, the LL equation (1) can be exactly recast as two DH equations [37]

$$\frac{\partial n}{\partial t} = \underbrace{\nabla \cdot [(1 - n^2)\mathbf{u}]}_{\text{spin current}} + \underbrace{\alpha(1 - n^2)\frac{\partial\Phi}{\partial t}}_{\text{spin relaxation}}, \qquad (3a)$$

$$\frac{\partial\mathbf{u}}{\partial t} = \underbrace{\nabla[(\sigma - |\mathbf{u}|^2)n]}_{\text{velocity flux}} - \underbrace{\nabla\left(\frac{\Delta n}{1 - n^2} + \frac{n|\nabla n|^2}{(1 - n^2)^2}\right)}_{\text{dispersion}}$$

$$- \underbrace{\nabla h_0}_{\text{potential force}} + \underbrace{\alpha\nabla\left(\frac{1}{1 - n^2}\nabla \cdot [(1 - n^2)\mathbf{u}]\right)}_{\text{viscous loss}}. \qquad (3b)$$

Equation (3a) is reminiscent of spin density continuity [42] from which we identify the spin density flux as the spin current

$$\mathbf{J}_s = -(1 - n^2)\mathbf{u}. \qquad (4)$$

Vacuum carries zero spin current. However, maximal spin current is reached when $n = 0$, identified as the saturation density. This implies that ferromagnetic textures ($\mathbf{u} \neq 0$) are better spin current conductors than small-amplitude spin waves [43]. The hydrodynamic equivalents for the fluid velocity Eq. (3b) are displayed. When $n = |\nabla h_0| = 0$, Eq. (3b) becomes $\partial\mathbf{u}/\partial t = \alpha\nabla(\nabla \cdot \mathbf{u})$, a diffusion equation for the velocity; hence, $\alpha > 0$ acts similar to a viscosity. Previous works [13–16] have neglected exchange dispersion and nonlinearity in Eqs. (3) by assuming the long-wavelength, near saturation density, low-velocity

limit, i.e., $|\nabla n| \ll 1$, $|n| \ll 1$, and $|\mathbf{u}|^2 \ll 1$. As we show below, the full nonlinearity and exchange dispersion included in Eqs. (3a) and (3b) are required to describe the existence and stability regions of magnetic hydrodynamic states and broken Galilean invariance.

Insight can be gained from the homogeneous field $\nabla h_0 \to 0$, conservative $\alpha \to 0$ limit, where Eqs. (3) become conservation laws for n and $\mathbf{u}$. Notably, the non-negative deviation from vacuum $(1 - n^2)$, or fluid density, is not conserved. A conservation law for the momentum $\mathbf{p} = n\mathbf{u}$ can also be obtained,

$$\frac{\partial\mathbf{p}}{\partial t} = \nabla \cdot [(1 - n^2)\mathbf{u}\mathbf{u}^T] + \nabla P(n, |\mathbf{u}|) + \nabla \cdot \left(\frac{\nabla n\nabla n^T}{1 - n^2}\right)$$

$$- \nabla\left(\frac{n\Delta n + \frac{1}{2}|\nabla n|^2}{1 - n^2} + \frac{n^2|\nabla n|^2}{(1 - n^2)^2}\right), \qquad (5)$$

where the magnetic pressure is defined as

$$P(n, |\mathbf{u}|) = \frac{1}{2}(1 + n^2)(\sigma - |\mathbf{u}|^2) - \sigma. \qquad (6)$$

Equations (3a) with $\alpha = 0$, and (5) are analogous to the time-reversed Euler equations expressing conservation of mass and momentum for a 2D, compressible, isentropic fluid with a density- and velocity-dependent pressure P.

Additionally, the one-dimensional conservative limit of Eqs. (3a) and (3b) are exactly the equations describing polarization waves in two-component spinor Bose gases [33,34] and, in the near vacuum ($|n| \sim 1$), long-wavelength, and low-frequency regime, approximate the mean field dynamics of a BEC [24,44]. This suggests that thin film ferromagnets are ripe for the exploration of nonlinear structures observed in BECs, e.g., "Bosenovas" [25,27] in attractive ($\sigma = -1$), and dark solitons [30], vortices [22], and DSWs [20] in repulsive ($\sigma = +1$) BECs. Some of these structures have been observed in uniaxial (dissipative droplets [5–7]) and planar (vortices [8]) thin film ferromagnets. As we demonstrate, hydrodynamic states are also supported.

Consider an ideal planar thin film ferromagnet ($\sigma = +1$) and a homogeneous field. Equations (3a) admit a static ($\partial\Phi/\partial t = 0$) solution with nonzero fluid velocity, $\mathbf{u} = u\hat{\mathbf{x}}$, $|u| < 1$, $n = 0$, and $h_0 = 0$. These are ground states known as spin-density waves (SDWs) [45] or soliton lattices [15] that minimize both exchange and anisotropy energies; i.e., any configuration with $|u| < 1$ is stable when $\mathbf{m}$ lies purely in plane. SDWs exhibit a periodic structure that affords them topological stability whereby the phase rotation can be unwound only by crossing a magnetic pole ($|n| = 1$) [15,37]. For a nonzero field, $|h_0| < 1 - u^2$, SDWs are also supported for any $|u| < 1$ when $n = h_0/(1 - u^2)$ due to the longitudinal spin density relaxation effected by Eq. (3a). Such a relaxation maintains u and thus the topology of and finite spin current carried by a SDW. This property is identical to that of equilibrium transverse spin currents in other magnetic textures including domain walls and vortices [Ref. [15], Eq. (4) in Ref. [46]].

For no damping, Eqs. (3) admit dynamic solutions parametrized by the constants $(\bar{n}, \bar{u})$, where $|\bar{n}| \leq 1$, $\mathbf{u} = \bar{u}\,\hat{\mathbf{x}}$, called the uniform hydrodynamic state (UHS). The fluid velocity $\bar{u}$ is the wave number of the UHS whose frequency $\Omega = d\Phi/dt$ is

$$\Omega(\bar{n}, \bar{u}) = -(1 - \bar{u}^2)\bar{n} + h_0, \qquad (7)$$

obtained from the magnetic equivalent of Bernoulli's equation $2P(\bar{n}, |\bar{u}|) + \bar{u}^2 + \bar{n}(\Omega - h_0) = -\sigma$ [37]. Here, positive $\bar{u}$ implies clockwise *spatial* increase of the azimuthal phase Φ, whereas negative Ω implies clockwise *temporal* precession about the $+\hat{\mathbf{z}}$ axis defining forward and backward wave conditions, schematically shown in Fig. 1. This is in contrast to magnetostatic forward and backward volume waves established by the relative direction between their wave vector and the external applied field.

The magnetization in a UHS can exhibit large angle deviations from the $+\hat{\mathbf{z}}$ axis, making it a strongly nonlinear texture. Near saturation density, $|\bar{n}| \ll 1$, a UHS limits to a spin superflow [14–16] whereas near vacuum, $\bar{n} \sim \pm 1$, the UHS frequency Eq. (7) becomes the exchange spin-wave dispersion $\Omega \sim \pm \bar{u}^2 + h_0 \mp 1$. Thus, a UHS is the generalization of periodic magnetic textures from large (spin superflow) to small (spin-wave) amplitudes. It is important to recognize that the ground state for the UHS is a SDW; i.e., the ground state of planar ferromagnets is not defined by a single orientation except for the vacuum state. In this sense, the UHS is significantly different from the conventional theory of linear and nonlinear spin waves based on the Holstein-Primakoff transformation [10,47] or nonlinear macrospin dynamics [11].

Small-amplitude perturbations of a UHS can be regarded as spin waves with a generalized dispersion relation obtained from the linearization of Eqs. (3a) and (3b),

$$\omega_{\pm}(\mathbf{k}, \mathbf{V}) = (2\bar{n}\mathbf{u} - \mathbf{V}) \cdot \mathbf{k} \pm |\mathbf{k}|\sqrt{(1 - \bar{n}^2)(1 - \bar{u}^2) + |\mathbf{k}|^2}, \qquad (8)$$
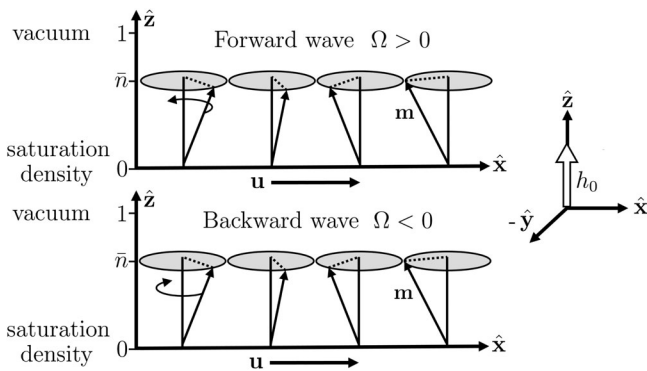
where $\mathbf{k}$ is the wave vector, and the velocity $\mathbf{V}$ reflects a Doppler shift, i.e., the velocity of an external observer with respect to the UHS. The dispersion relation shows that magnetic systems lack Galilean invariance. In other words, an observer velocity $\mathbf{V} \propto \mathbf{u}$ does not generally result in a reference frame where the relative fluid velocity is zero. Galilean invariance is recovered near vacuum ($|\bar{n} \approx 1|$) with dispersion $\omega_{\pm}(\mathbf{k}, \mathbf{V}) = (2\mathbf{u} - \mathbf{V}) \cdot \mathbf{k} \pm |\mathbf{k}|^2$, i.e., exchange-mediated spin waves and the BEC limit [24,44]; and for spin superflow ($\bar{n} \approx 0$), $\omega_{\pm}(\mathbf{k}, \mathbf{V}) = -\mathbf{V} \cdot \mathbf{k} \pm |\mathbf{k}|\sqrt{1 + |\mathbf{k}|^2}$. Importantly, the fluid velocity $\bar{u}$ confers a spectral shift in Eq. (8) due to the UHS's intrinsically chiral topology, similar to the interfacial Dzyaloshinskii-Moriya interaction [48].

The long wavelength limit of Eq. (8) leads to coincident spin-wave phase and group velocities, i.e., magnetic sound velocities,

$$s_{\pm} = 2\bar{n}\,\bar{u} + \bar{V} \pm \sqrt{(1 - \bar{n}^2)(1 - \bar{u}^2)}. \qquad (9)$$

Here, we assume $\mathbf{V}$ collinear and opposite to $\mathbf{u}$ ($\mathbf{V} = -\bar{V}\,\hat{\mathbf{x}}$). Subsonic flow occurs when spin waves can propagate both forward and backward: $s_- < 0 < s_+$. However, when $0 < s_- < s_+$, the flow is supersonic and some spin waves are convected away. These conditions can be quantified in terms of the Mach numbers M_u, M_V when $\bar{V} = 0$, $\bar{u} = 0$, respectively,

$$M_u = |\bar{u}|\sqrt{\frac{1 + 3\bar{n}^2}{1 - \bar{n}^2}}, \qquad M_V = \frac{|\bar{V}|}{\sqrt{1 - \bar{n}^2}}. \qquad (10)$$

For both, the flow is subsonic or laminar when $M < 1$. In the supersonic regime, $M > 1$, it is energetically favorable to generate spin waves, thus leading to the Landau breakdown of superfluidlike flow [49]. The resulting phase diagrams are shown in Fig. 2. Interestingly, Eq. (10) predicts that M is
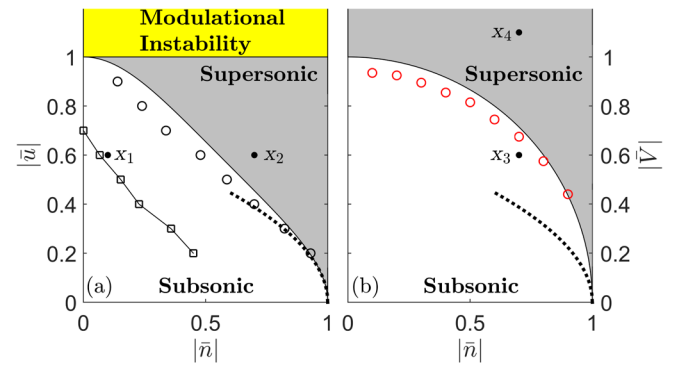

FIG. 2. UHS phase diagram for (a) $\bar{V} = 0$ and (b) $\bar{u} = 0$ with subsonic (white), supersonic (gray), and modulationally unstable (yellow) regimes. Circles are micromagnetic calculations of the sonic curves $M_u = 1$ and $M_V = 1$. The BEC-limit regime sonic curve is dashed. Open squares represent the micromagnetically calculated sonic curve of a width $w = 20$, thickness $\delta = 1$ nanowire including nonlocal dipolar fields and $T = 300$ K thermal field. Selected simulation conditions are denoted by x_1 to x_4.

FIG. 1. Schematic of the magnetization rotation of a UHS. The longitudinal spin density is the vertical axis limited by vacuum ($|n| = 1$) and saturation density ($n = 0$). Forward and backward wave conditions are determined by the sign of the frequency Ω.

independent of h_0, implying that only the UHS longitudinal spin density and its nontrivial topology, $\bar{u}$, set the supersonic transition, not the frequency Ω. It must be noted that broken Galilean invariance causes the standard Landau criterion concept $\bar{u} < \min[s_\pm]$ [24] to give an incorrect sonic curve.

A qualitatively distinct flow regime occurs when $|\bar{u}| > 1$ and the sound velocities Eq. (9) are complex. This corresponds to a change in the mathematical type of the long wavelength Eqs. (3) from hyperbolic (wavelike) to elliptic (potential-like). Consequently, the UHS is unstable in the sense that small fluctuations lead to drastic changes in its temporal evolution or modulational instability (MI) [50,51]. Note that $|\bar{u}| < 1$, $|\bar{V}| > 1$ does not result in MI.

The aforementioned regimes were validated by performing micromagnetic simulations with damping [12]. We simulate dynamics for an ideal Permalloy nanowire ($\mu_0 M_s = 1$ T) of nondimensional width $w = 20$ with transverse free spin boundary conditions and horizontal periodic boundary conditions (PBCs). We initialize with a SDW, include only local dipolar fields (zero thickness limit), and set $\alpha = 0.01$. A homogeneous field h_0 stabilizes the SDW at a specific $\bar{n}$ and a quantized $\bar{u}$ that satisfies the PBC. This enables us to numerically probe along a horizontal line in the phase diagram of Fig. 2(a) by implementing a slowly increasing h_0. By inserting a point defect (a magnetic void), the SDW spontaneously generates spin waves when $\bar{n}$ is large enough to cross the supersonic transition, leading to a breakdown in the spatial homogeneity of the SDW [37]. Because of the SDW's topology and the PBC, the change in symmetry is accommodated by annihilating a single 2π phase rotation and reducing $\bar{u}$ in a quantized fashion. Topologically, this is possible in planar ferromagnets by crossing a magnetic pole, e.g., nucleating a vortex, as shown in the Supplemental Material, video 1 [37]. This was also observed in wires of width $w = 40$. The sonic curve estimated this way is shown in Fig. 2(a) by black circles, demonstrating good agreement with $M_u = 1$. We attribute any discrepancy to boundary and finite size effects [52], as further explored below.

We use the same numerical method described above with the addition of thermal fluctuations and the symmetry-breaking nonlocal dipolar fields to study the stability of a SDW in a nanowire of nondimensional thickness $\delta = 1$. In this case, the SDW topological structure completely collapses at the boundary shown in Fig. 2(a) by squares. In contrast to a recent report where stable spin superflow was predicted only for nanowires shorter than the material exchange length [18], we observe stable SDWs over a wide range of parameters in phase space (Supplemental Material, video 2 [37]).

The supersonic transition in the moving frame is estimated by use of a numerical method described elsewhere [53]. A moving, perpendicular, localized, weak magnetic field spot with velocity $\bar{V}$ is used to perturb a homogeneous state in the bias field $h_0 = \bar{n}$. The obtained sonic curve is in good agreement with $M_V = 1$, red circles in Fig. 2(b).

We now explore the effect of finite-sized obstacles on a UHS. As observed in BECs, obstacles can generate vortices, wave fronts, and DSWs in a fluid flow [20–22]. Note that wave fronts, i.e., "spin-Cherenkov" radiation, were previously observed via micromagnetic simulations in homogeneous ($\bar{u} = 0$), thick ferromagnets in the moving reference frame ($\bar{V} \neq 0$) [54]. The wave fronts studied here are different, resulting from both moving ($\bar{u} = 0$, $\bar{V} \neq 0$) and static ($\bar{u} \neq 0$, $\bar{V} = 0$) reference frames, yet another manifestation of broken Galilean invariance. We illustrate these features with simulations where $\alpha = 0.01$ and local dipolar fields are included, shown in Fig. 3 as a gray scale map and vector field for n and $\mathbf{u}$, respectively (see Supplemental Material [37] for the corresponding in-plane magnetization map). First, we consider the stable subsonic condition x_1 of Fig. 2(a) for a SDW in the static reference frame $(\bar{n}, \bar{u}) = (0.1, 0.4)$ with a magnetic defect within a circular area of $\pi/\bar{u}$ in diameter. The static configuration in Fig. 3(a) is analogous to Bernoulli's principle for laminar flow.

A different situation occurs at the supersonic condition x_2 $(\bar{n}, \bar{u}) = (0.7, 0.6)$, Fig. 3(b). Here, the density develops a
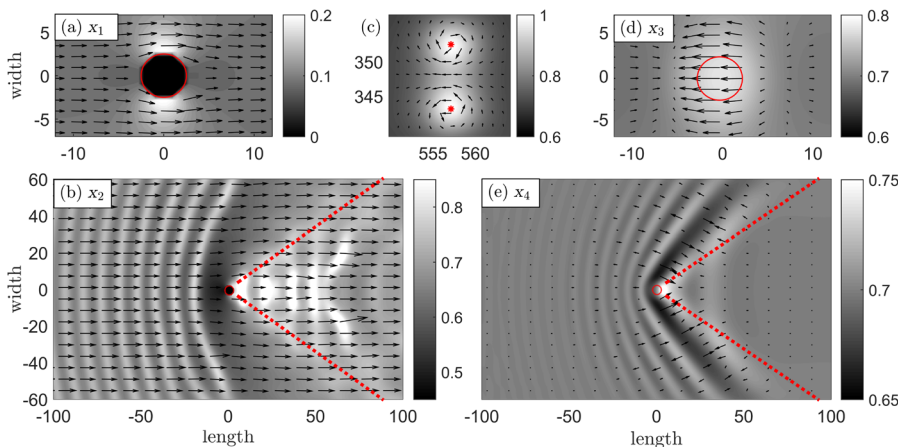

FIG. 3. Snapshots of a (a), (b) SDW flowing past a stationary magnetic defect ($\bar{V} = 0$) and; (d), (e) a homogeneous state subject to a moving, localized magnetic field ($\bar{V} \neq 0$) with longitudinal spin density n (gray scale map) and velocity field $\mathbf{u}$ (arrows). The simulation region is much larger than what is visible. The defect or localized magnetic field position is shown by a red circle. For subsonic conditions, (a) and (d), the flow is static and laminar. In supersonic flow, (b) and (e), a Mach cone (dashed) and static wave fronts are observed. Propagating vortex-antivortex pairs with cores (asterisks) generated in (b) are shown in (c), far from the defect as opposite circulations of the velocity field (background $\bar{u} = 0.6$ is subtracted).

distinct Mach cone (dashed), delimiting static wave fronts and the nucleation of propagating vortex-antivortex pairs, shown far from the defect in Fig. 3(c). In the moving reference frame, a homogeneous state is perturbed by a moving, weak, localized field. Utilizing the subsonic condition x_3 $(\bar{n}, \bar{u}, \bar{V}) = (0.7, 0, 0.6)$, the flow is laminar, Fig. 3(d) [cf. supersonic x_2 in Fig. 2(a)]. Wave front radiation outside the Mach cone is observed for the supersonic condition x_4 $(\bar{n}, \bar{u}, \bar{V}) = (0.7, 0, 1.1)$ in Fig. 3(e). However, the field spot amplitude is too weak to excite vortex-antivortex pairs. Animations are in the Supplemental Material, videos 3–6 [37].

The MI regime for UHSs with $|\bar{u}| > 1$ exhibits a violent instability (see Supplemental Material, video 7 [37]). Notably, for a uniaxial ferromagnet with $\sigma = -1$, MI is *always* operative. This is consistent with the focusing of spin waves and the formation of dissipative droplets in spin torque devices utilizing materials with perpendicular magnetic anisotropy [4–7].

We now discuss an experimental test for the hydro-dynamic predictions. As mentioned above, the dispersion relation Eq. (8) features a spectral shift with nonzero fluid velocity. This shift can be observed, e.g., by means of Brillouin light scattering (BLS), as already shown for Dzyaloshinskii-Moriya interactions [48]. For a given fluid velocity, the magnitude of the shift, $2\bar{n}\,\bar{u}$, can be tuned by an externally applied field. Use of such tuning, in combi-nation with BLS, will allow a direct test of the predicted breaking of Galilean invariance, insofar as the nonlinear properties of the dispersion relation Eq. (8) can be quanti-tatively investigated. In particular, if one plots spin-wave frequency vs wave number squared for both the Stokes and anti-Stokes BLS peaks in the short-wavelength limit, $|\mathbf{k}| \gg (1 - \bar{n}^2)(1 - \bar{u}^2)$, the modulus of the zero wave number intercepts from linear regression will not be equal in the case of broken Galilean invariance, in contrast to the case of Galilean invariance, where the intercepts would be equal.

In summary, the dispersive hydrodynamic formulation permits us to quantify the manner in which thin film ferromagnets lack Galilean invariance in the context of linear spin wave propagation on a dynamic UHS or static SDW background. The breaking of Galilean invariance is often associated with relativistic phenomena, wherein the Lorentz transformation conjoins space-time into a single coordinate system, replacing the Galilean transformation. Instead, the present case ultimately reflects the counterin-tuitive ability of exchange-coupled, topological spin textures to support spin currents, even in the static case. The predictions are robust to damping, nonlocal dipolar fields, and finite temperatures for a large portion of phase space. The exact representation of the LL equation in DH form, along with associated mathematical tools [23,31,50], enables new magnetodynamic predictions and a frontier of magnetic research, for example, the observation of a Mach cone, wave

fronts, and vortex nucleation. In addition, the form of the DH equations suggests the existence of coherent structures such as oblique solitons and DSWs.

———————————

[*] ezio.iacocca@colorado.edu

[1] L. Berger, Phys. Rev. B **54**, 9353 (1996).

[2] J. C. Slonczewski, J. Magn. Magn. Mater. **159**, L1 (1996).

[3] K. M. D. Hals and A. Brataas, Phys. Rev. B **88**, 085423 (2013).

[4] M. A. Hoefer, T. J. Silva, and M. W. Keller, Phys. Rev. B **82**, 054432 (2010).

[5] S. M. Mohseni, S. R. Sani, J. Persson, T. N. A. Nguyen, S. Chung, Y. Pogoryelov, P. K. Muduli, E. Iacocca, A. Eklund, R. K. Dumas, S. Bonetti, A. Deac, M. A. Hoefer, and J. Åkerman, Science **339**, 1295 (2013).

[6] F. Macià, D. Backes, and A. Kent, Nat. Nanotechnol. **10**, 1038 (2014).

[7] S. Chung, A. Eklund, E. Iacocca, S. Mohseni, S. Sani, L. Bookman, M. A. Hoefer, R. Dumas, and J. Åkerman, Nat. Commun. **7**, 11209 (2016).

[8] Q. Mistral, M. van Kampen, G. Hrkac, J.-V. Kim, T. Devolder, P. Crozat, C. Chappert, L. Lagae, and T. Schrefl, Phys. Rev. Lett. **100**, 257201 (2008).

[9] A. Slavin and V. Tiberkevich, IEEE Trans. Magn. **45**, 1875 (2009).

[10] V. L'vov, *Wave Turbulence under Parametric Excitation* (Springer, New York, 1994).

[11] G. Bertotti, I. Mayergoyz, and C. Serpico, *Nonlinear Magnetization Dynamics in Nanosystems*, 1st ed. (Elsevier Science, New York, 2008).

[12] A. Vansteenkiste, J. Leliaert, M. Dvornik, M. Helsen, F. Garcia-Sanchez, and B. Van Waeyenberge, AIP Adv. **4**, 107133 (2014).

[13] B. Halperin and P. Hohenberg, Phys. Rev. **188**, 898 (1969).

[14] J. König, M. C. Bønsager, and A. H. MacDonald, Phys. Rev. Lett. **87**, 187202 (2001).

[15] E. B. Sonin, Adv. Phys. **59**, 181 (2010).

[16] S. Takei and Y. Tserkovnyak, Phys. Rev. Lett. **112**, 227201 (2014).

[17] H. Chen, A. D. Kent, A. H. MacDonald, and I. Sodemann, Phys. Rev. B **90**, 220401 (2014).

[18] H. Skarsvåg, C. Holmqvist, and A. Brataas, Phys. Rev. Lett. **115**, 237201 (2015).

[19] B. Flebus, S. A. Bender, Y. Tserkovnyak, and R. A. Duine, Phys. Rev. Lett. **116**, 117201 (2016).

[20] M. A. Hoefer, M. J. Ablowitz, I. Coddington, E. A. Cornell, P. Engels, and V. Schweikhard, Phys. Rev. A **74**, 023623 (2006).

[21] I. Carusotto, S. X. Hu, L. A. Collins, and A. Smerzi, Phys. Rev. Lett. **97**, 260403 (2006).

[22] A. L. Fetter, Rev. Mod. Phys. **81**, 647 (2009).

[23] G. El and M. Hoefer, Physica (Amsterdam) **333D**, 11 (2016).

[24] C. Pethick and H. Smith, *Bose-Einstein Condensation in Dilute Gasses* (Cambridge University Press, Cambridge, England, 2002).

[25] E. A. Donley, N. R. Claussen, S. L. Cornish, J. L. Roberts, E. A. Cornell, and C. E. Wieman, Nature (London) **412**, 295 (2001).

[26] G. A. El, A. Gammal, and A. M. Kamchatnov, Phys. Rev. Lett. **97**, 180405 (2006).

[27] S. L. Cornish, S. T. Thompson, and C. E. Wieman, Phys. Rev. Lett. **96**, 170401 (2006).

[28] Y. G. Gladush, G. A. El, A. Gammal, and A. M. Kamchatnov, Phys. Rev. A **75**, 033619 (2007).

[29] P. G. Kevrekidis, D. J. Frantzeskakis, and R. Carretero-Gonzàlez, *Emergent Nonlinear Phenomena in Bose-Einstein Condensates: Theory and Experiment* (Springer, Berlin, 2008).

[30] D. J. Frantzeskakis, J. Phys. A **43**, 213001 (2010).

[31] P. G. Kevrekidis, D. J. Frantzeskakis, and R. Carretero-González, *The Defocusing Nonlinear Schrödinger Equation* (SIAM, Philadelphia, 2015).

[32] S. Demokritov, V. Demidov, O. Dzyapko, G. A. Melkov, A. A. Serga, B. Hillebrands, and A. Slavin, Nature (London) **443**, 430 (2006).

[33] C. Qu, L. P. Pitaevskii, and S. Stringari, Phys. Rev. Lett. **116**, 160402 (2016).

[34] T. Congy, A. M. Kamchatnov, and N. Pavloff, SciPost Phys. **1**, 006 (2016).

[35] G. Beach, M. Tsoi, and J. Erskine, J. Magn. Magn. Mater. **320**, 1272 (2008).

[36] K. Yamada, S. Kasai, Y. Nakatani, K. Kobayashi, H. Kohno, A. Thiaville, and T. Ono, Nature (London) **6**, 269 (2007).

[37] See Supplemental Material http://link.aps.org/supplemental/10.1103/PhysRevLett.118.017203 for further details on the DH derivation, micromagnetic simulations, and topology of hydrodynamic states, which includes Refs. [38,39].

[38] M. Sparks, *Ferromagnetic Relaxation Theory* (McGraw-Hill, New York, 1965).

[39] H.-B. Braun, Adv. Phys. **61**, 1 (2012).

[40] S. K. Kim, S. Takei, and Y. Tserkovnyak, Phys. Rev. B **92**, 220409 (2015).

[41] N. Papanicolaou and T. Tomaras, Nucl. Phys. **B360**, 425 (1991).

[42] S. Zhang and Z. Yang, Phys. Rev. Lett. **94**, 066602 (2005).

[43] A. Hoffmann, IEEE Adv. Magn. **49**, 5172 (2013).

[44] I. I. Satija and R. Balakrishnan, Phys. Lett. A **375**, 517 (2011).

[45] G. Grüner, Rev. Mod. Phys. **66**, 1 (1994).

[46] Y. Tserkovnyak, E. M. Hankiewicz, and G. Vignale, Phys. Rev. B **79**, 094415 (2009).

[47] D. C. Mattis, *The Theory of Magnetism Made Simple* (World Scientific, Hackensack, NJ, 2006), p. 82.

[48] H. T. Nembach, J. M. Shaw, M. Weller, E. Jué, and T. J. Silva, Nat. Phys. **11**, 825 (2015).

[49] L. D. Landau, Phys. Rev. **60**, 356 (1941).

[50] G. B. Whitham, *Linear and Nonlinear Waves* (John Wiley & Sons, New York, 1974).

[51] V. Zakharov and L. Ostrovsky, Physica (Amsterdam) **238D**, 540 (2009).

[52] T. Frisch, Y. Pomeau, and S. Rica, Phys. Rev. Lett. **69**, 1644 (1992).

[53] M. Hoefer and M. Sommacal, Physica (Amsterdam) **241D**, 890 (2012).

[54] M. Yan, A. Kákay, C. Andreas, and R. Hertel, Phys. Rev. B **88**, 220412 (2013).